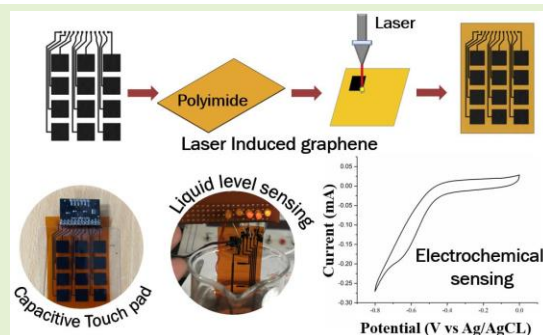


# Laser-Induced Flexible Electronics (LIFE) for Resistive, Capacitive and Electrochemical Sensing Applications

Avinash Kothuru, C. Hanumanth Rao, Puneeth S B, Mary Salve, Khairunnisa Amreen and Sanket Goel\*, Senior Member, IEEE  
MEMS, Microfluidics and Nanoelectronics laboratory, Department of Electrical and Electronics Engineering, Birla Institute of Technology and Science, Pilani, Hyderabad Campus, Hyderabad, India.

**Abstract**—Engineering a cost-effective, flexible electronic device in a one-step fabrication process is quite challenging to perform. Herein, we have introduced a simple, low-cost, solid-state process for producing and printing of complex circuits using Laser-Induced Graphene (LIG). In the present work, LIG has been effectively and selectively formed from direct CO<sub>2</sub> laser ablation on a polyimide sheet. Varying CO<sub>2</sub> laser power and speed, the electrical conductivity of the LIG has shown a linear increment in the conductivity measurement. The laser-induced samples were structurally characterized using Scanning Electron Microscopy (SEM), EDX, X-ray Photoelectron Spectroscopy (XPS), Raman spectroscopy. The results show a one-step method to create Graphene-derived structures on the polyimide sheet surface. This method of generating LIG on a flexible substrate (polyimide sheet) offers an easy way to fabricate Laser-Induced Flexible electronics (LIFE) circuits. Using this, the feasibility and the realization of a capacitive touch sensor and liquid level sensor has been successfully demonstrated. Further, as a prototype system, the LIG was examined for the H<sub>2</sub>O<sub>2</sub> electrochemical sensing application. It gives an appreciable response for the detection of H<sub>2</sub>O<sub>2</sub> in comparison to other carbon-based electrodes with limit-of-detection (LOD) as 0.3 μM in a linear range from 1 μM to 10 μM.

**Index Terms**— Laser-Induced Flexible Electronics (LIFE), Polyimide, electrochemical sensing, Touchpad, water-level monitoring.



## I. INTRODUCTION

Electronics has become so dominant and dependable that it is continuously harnessed in many ongoing research domains to realize cost-effective, user-friendly and robust devices with better accuracy and precision. Since their inception, the electronic circuits were bulky as they were realized on the dotted circuit boards, with a manual and time-consuming process. Later on, a thin copper sheet based Printed Circuit Boards (PCB) were developed, which has brought remarkable changes to modern electronics. On PCB, the copper conductive traces were obtained by a well-established subtractive chemical wet-etching process. Even though such a PCB fabrication process is well-established, but there is a huge scope to make it automated, additive, and cost-and-time efficient. Further, the PCB fabrication process involves complex fabrication method that includes carcinogenic chemicals, and hot soldering is necessarily leading to another significant concern. In few cases, such as packaging of the circuit, stacking of Integrated Circuits (IC), electrical

connection between the stacks of circuit boards, rigid PCB have disadvantages, leading to the requirement of the flexible boards [1]–[3]. Hence, an alternative technique is necessary to create electronic circuits on a flexible surface, which reduces the area and increases the application potential of the device.

The flexible electronics has been reported for many applications in day-to-day life, includes connectors for flexible displays, contacts in keypads, keyboards, health monitoring devices and much more[4][5][6][7][8]. Such flexible electronic devices have been fabricated by popular approaches such as screen-printing and inkjet printing, where suitable conductive ink, developed using Carbon or Silver, was employed to get the conductive traces. These traces are formed on many substrates such as polymeric film, polyethylene terephthalate (PET), polyimide (PI) and can be easily connected on an onboard PCB. This approach is shown in stacking of PCBs, resulting in the reduction of the area to realize the necessary circuit. These traces can be connected to the PCB using Flexible Printed Electronic Circuit connector, or card edge connector[9]. These genres of flexible circuits play a prominent role to develop sensors, Radio-frequency

identification (RFID), flexible displays and antennas. In recent times, the compositions of conductive inks were achieved using many novel materials, such as nanoparticle, nanowires and graphene sheets, to increase the conductivity. The conductive inks were prepared by mixing conductive material with solvents to maintain the consistency based on the requirement. However, the main challenge in developing such inks is to properly synthesize the nanomaterials itself and the bonding process after solidification[10]. Other drawbacks of these methods are clogging of nozzles of the inkjet printers, preparation of stencils for screen-printing, complicated and tedious process for obtaining nanoparticles. These challenges increase the time to obtain the flexible circuits, an increase in cost and non-uniformity of the conductance of the circuit.

Various nanomaterials fabrication techniques are proposed during recent years, which includes nanoparticles, Nano-rods of materials such as copper, silver, gold, platinum that have high conductive properties. The CO<sub>2</sub> laser method is being used widely for obtaining the carbon on polyimide sheet[11]. An alternative process is synthesizing of Graphene, an allotrope of carbon, which has immense advantages due to its physical, chemical, mechanical and electrical properties. The graphene is a three-dimensional porous structure with very few layers (3-5 layers); this ensures flexibility, high surface area and mechanical endurance[12]. However, the major challenge exists in obtaining a few layers of graphene. As the number of layers increases, the properties change which may result in different carbon allotropes such as Graphene oxide, reduced Graphene oxide, and Graphite. Due to the advantages as mentioned above, the applications of graphene are seen in various domains including storage of electrical energy as a supercapacitor, on electrode surface reversibility of absorption and desorption of electrolytic ions. The well-established procedures to fabricate crystalline graphene structures are oxidative acid synthesis route, chemical vapour deposition on thin films of Cu and Ni at elevated temperatures leading to porous material deposition[13]. This film of graphene can be transferred from one surface to the other transfer methods involving either a wet or dry process[14]. One of the reported drawbacks with the processes of forming reduced GO is that the quality of the graphene obtained does not remain the same as of native graphene[15].

One of the innovative and straightforward process to obtain graphene or graphene oxide has been demonstrated by focusing high energy density laser beam on to the surface of the substrates. This was achieved by ablating substrates under CO<sub>2</sub> laser in the desired pattern, designed in software as per the requirement, and fed to the CO<sub>2</sub> laser equipment[16]. The CO<sub>2</sub> laser ablation was been reportedly performed on different non-flexible substrates such as bread slice, coconut shell, various kinds of wood and much more. A similar process has been repeated on a flexible substrate, like polyimide (PI), whereby the traces of carbon was observed [17][18]. This process is famously known as Laser-Induced Graphene (LIG)[19]. The obtained samples were subjected to physico-chemical characterization techniques, such as XPS spectra, Raman Spectroscopy[20] and Scanning Electron Microscope (SEM)[21], and provided sufficient justification to conclude that the obtained carbon traces were of graphene oxide.

Since the present approach has been carried out on a hydrophobic polyimide substrate, therefore, it will be easily compatible with subsequent material processing. In this work, an optimized process has been demonstrated to create LIGs on a polyimide sheet using a low-power CO<sub>2</sub> laser. Rigorous characterizations were carried out to support the feasibility to employ such LIGs to create LIFE components for sensing applications. T. han et al reported in 2019, with speed and power of CO<sub>2</sub> laser the polyimide sheet was ablated and used as real time strain sensing[22]. To realize the potential and scope of such LIFE devices, varied applications like capacitive touchpad, electrochemical sensing and resistive liquid level sensor is demonstrated.

## II. Materials and Methods

Polyimide sheet of 125  $\mu\text{m}$  thickness was purchased from Dali Electronics, and a 30 W CO<sub>2</sub> Laser (Universal Laser Systems, VLS 3.60) was utilized to obtain the Laser-Induced Graphene (LIG) conductive traces. Hydrogen peroxide (30%) was procured from Sigma Aldrich and other basic chemicals of analytical grade were used. The topographical morphology and elemental analysis of the obtained CO<sub>2</sub> laser-induced graphene (LIG) were characterized by Scanning Electron Microscope (SEM) and Energy Dispersive Spectroscopy (EDS) techniques using Apreo Scanning Electron Microscope (SEM) from Thermo Fisher Scientific. Fourier transform infrared spectrometer instrument (FTIR-4200 from Jasco) was used to examine the samples for identifying the functional groups (organic or inorganic). In further, Witec Alpha 500 confocal Raman microscopy was used for the characterization. A Thermo scientific K-Alpha X-ray Photoelectron Spectrometer (XPS) instrument was utilized to examine the samples for surface analysis. For conductivity, resistance, resistivity measurement, Ossila machine, based on the Four-point probe mechanism was used. All the cyclic voltammetry (CV) measurements were performed using Bio-logic (SP-150) electrochemical workstation in a standard three-electrode configuration.

## III. Exerimental Procedure

### A. Formation of Laser-Induced Graphene(LIG) on Polyimide sheet

A basic design was drawn using AutoCAD Fusion 360, and the file was saved in .dxf format. The .dxf file was transferred in CorelDraw X7, and the outline width of the design was changed according to the preference of the CO<sub>2</sub> laser. As shown in Fig 1, by varying the speed and power, of the CO<sub>2</sub> laser, Laser-Induced Graphene (LIG) was obtained on polyimide (PI) [23], LIG reaches its highest crystallinity by laser power amplification[24][25]. Literature reports fabrication of LIG using CO<sub>2</sub> laser machine by varying the power and speed on PI, wherein conductivity is obtained and calculated. For instance, Lin et. al. induced 60W CO<sub>2</sub> laser on PI by varying power from 2.4 W to 5.4 W, showing the high conductivity of 25 S/cm at a power of 5.4 W. In present work, for 5.4 W laser power has 91.3% of carbon, 7.7% of oxygen

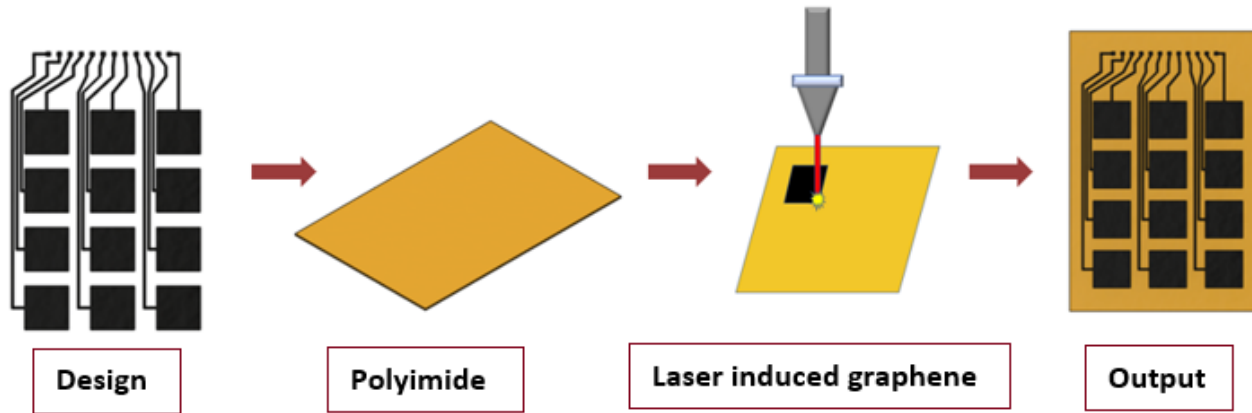


Fig 1 Schematic process to create Laser-Induced Graphene (LIG) structure on Polyimide

and 1.0% of nitrogen was observed. In the present study, above 95% of carbon was observed by varying 30 W CO<sub>2</sub> laser power from 1.35 W to 1.95 W as shown in Table I.

In general, by optimizing the laser power, the LIG thickness increased improving its conductivity.

### B. Capacitive Touchpad

By touching a capacitive touchpad, an amount of charge is drawn to the contact point which becomes functional. The change in the electrostatic field is calculated to determine the location. In this work, touchpads were designed with different approaches such as resistive and capacitive, whereby the capacitance-based touchpad has seen the upper hand in terms of extensive usage. The electrode patterns were created to act as touchpads with a particular pre-defined pattern. These patterns obtained on the PI sheet with the help of CO<sub>2</sub> laser was integrated along with the ICs, meant to detect the change in the capacitance, which was used along with a microcontroller and a display unit.

### C. Liquid level sensor

These sensors are used to detect liquid levels or interfaces between liquids such as water and oil. Level sensors calculate within the range. Level sensor shows whether the fluids are above or below the point of sensation. Level detection sensors can detect the fluid level in a container, and therefore, they have ample scope in real-life applications. Herein, an electronic-based approach was explored. LEDs were used to show the level, which was one of the natural and visual approaches to exhibit.

### D. Electrochemical sensing

A conventional three-electrode system consisting of a working electrode, a counter electrode, and a reference electrode is used for electrochemical sensing. Herein, the laser-induced graphene (LIG) sample was used as a working electrode, Ag/AgCl as reference and platinum as a counter. Cyclic voltammetry (CV) experiments were performed using 0.2 M phosphate buffer solution (PBS) pH 7 and 500 μM H<sub>2</sub>O<sub>2</sub> sample.

## IV. Material characterization

In order to interpret the surface morphology and structure of the LIG, samples were exposed to various physico-chemical and microscopic characterization like SEM, EDX, XRD analysis, XPS and Raman Spectroscopy[26].

### A. Scanning Electron Microscopy (SEM) and Dispersive X-ray Spectroscopy (EDX)

The Surface morphology study of the formed LIG on polyimide sheet was explored using scanning electron microscopy (SEM). Fig 2 exhibits SEM images of PI sheet before and after exposing to the CO<sub>2</sub> laser machine. Fig 2. (a - c) Clearly depicts the bare polyimide sheet without laser ablation, whereas, in Fig 2 (b-d), represents post exposure to CO<sub>2</sub> laser. An evident deposition of graphitic like framework was observed authenticating the LIG formation. Fig 2 (e) shows the EDX of a LIG sample. From the EDX, the carbon content in the LIG is above 95%, and oxygen content is near to 4%. Table 1 depicts the elemental analysis of the LIG [27].

TABLE I  
CARBON & OXYGEN CONTENT IN EACH SAMPLES

Elements	Bare PI	Sample 1	Sample 2	Sample 3	Sample 4	Sample 5
Carbon (%)	79.97	96.25	96.20	96.22	96.50	96.55
Oxygen (%)	20.03	3.75	3.8	3.78	3.5	3.45



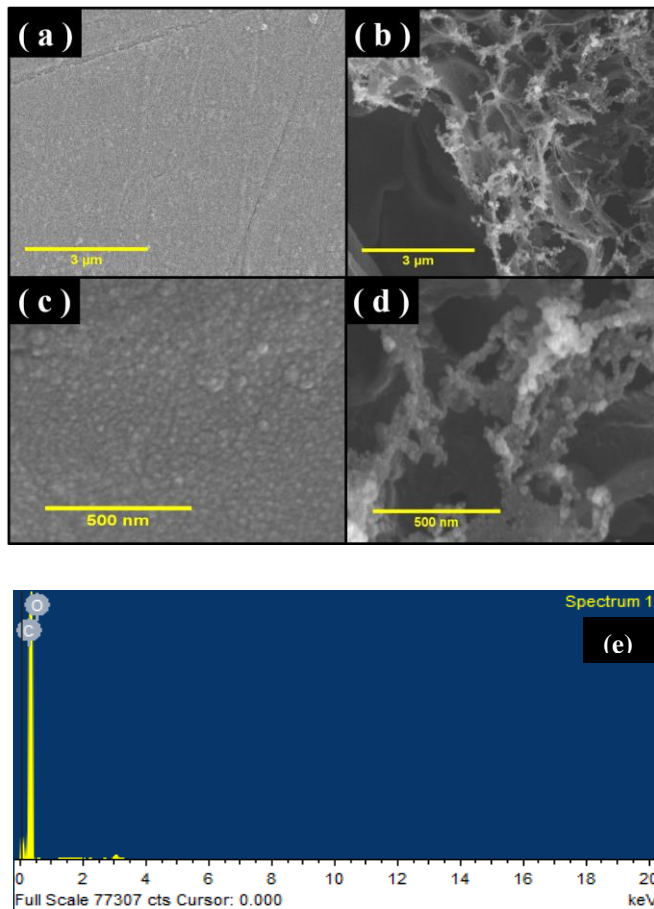


Fig 2. SEM images of (a-c) bare polyimide, (b-d)LIG sample after exposing to the CO<sub>2</sub> laser, (e) EDX of LIG sample showing carbon and oxygen peak

### B. X-ray Photoelectron Spectroscopy (XPS)

Varying the speed and power of the CO<sub>2</sub> laser, various samples were prepared. XPS C 1s spectrum analysis for all the samples was done. The peak values for the five samples are represented in Table 2. Fig 3. shows the XPS spectrum of the prepared Graphene Oxide (GO). From the literature [28][29], the deconvolution of GO peak happens at 284.6, 286.6 and 288.5eV. The number of counts per second depends on the concentration of the elements present in the compound. For the LIG sample, the binding energies of the corresponding functional group gives different counts per second with respect to the concentration present in the sample.

TABLE II  
XPS C 1 S SPECTRUM OF LIG SAMPLE

Samples	Counts/s	Binding energy (eV)
1	265713	284.38
2	138620	284.78
3	170895	284.78
4	248508	284.68
5	241663	284.58

For the LIG sample, the C 1s XPS spectrum peaks after the deconvolution, are at 284.67, 286.55 and 288.48 eV, similar to the reported values. The peak values represent a functional group of C-C, O-C=O, and sp<sup>2</sup>. Here, without deconvolution, some samples show a peak at 284.78 that is near to sp<sup>3</sup> carbon. The C 1s XPS spectrum intensity peaks manifest that it contained only C and O elements indicating the absence of impurities.

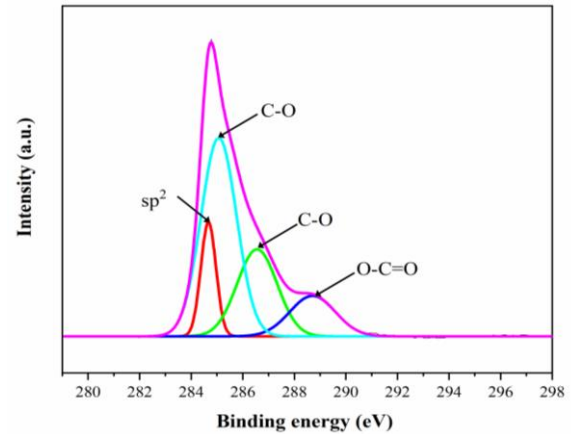


Fig 3. XPS of graphene oxide

### C. Raman Spectroscopy

Investigation of the obtained LIG was carried out using Raman Spectroscopy to make sure that the material was carbon allotropes. Five LIG samples were characterized using Raman spectroscopy (varying speed and power), and the Raman peaks are illustrated in Fig 4. and Table 3. The results for the intensity of G bands, D bands and 2D bands are shown in Table 3.

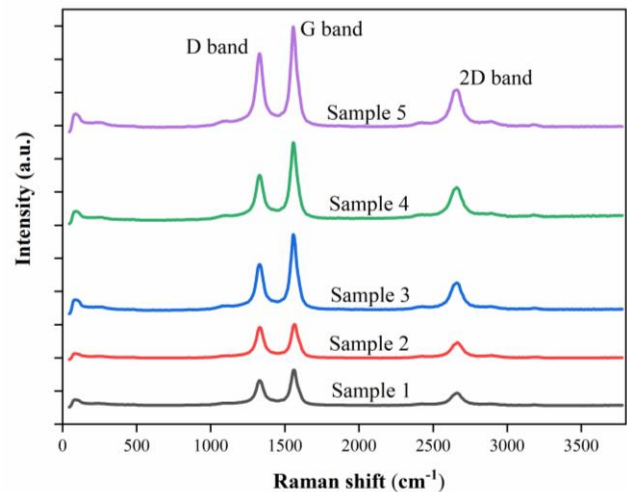


Fig 4. Raman spectra of Graphene oxide for five samples varying speed and power

The disordered carbon structure can be represented by the intensity ratio of the G band to the D band ( $I_D/I_G$ )[23][30]. The  $I_D/I_G$  ratio of the as prepared LIG samples varied between 0.668 and 0.942, indicating the varying carbon structural defects in the lattice structure of various LIG samples. Raman results for five samples show the same D and G band wavelength, i.e. 1330.039 cm<sup>-1</sup> and 1557.68 cm<sup>-1</sup>. Therefore, based on the values obtained it can be concluded that the

samples had a formation of graphene oxide. As the ratio,  $I_{2D}/I_G$ , manifest the number of graphene layers, the variation of the number of layers should be one of the reasons behind the variation in electrical conductivity for various LIG samples.

TABLE III  
D AND G BANDS FOR THE LIG SAMPLES

S.no	D Band	G Band	2D Band	$I_D/I_G$	$I_{2D}/I_G$
1	658.33	818.30	468.36	0.805	0.572
2	743.58	789.55	513.94	0.942	0.651
3	1007.61	1462.30	727.80	0.689	0.498
4	995.83	1490.11	810.22	0.668	0.544
5	1446.41	1849.08	898.80	0.782	0.486

#### D. Conductivity Test (Four-Point Probe System)

The prepared LIG samples were tested for conductivity by placing them at the center of the four-probe system. To measure the conductivity, the input of a maximum 5 V with 0.01 V increment and 25 repetitions were carried out. Fig 5. (a) shows the plot between applied voltage (V) and measured current (A), and Fig 5 (b) shows the plot between applied current (A) and measured voltage (V). As can be seen, the conductivity of the sample changes with varying speed and power of laser on the polyimide sheet.

TABLE IV  
CONDUCTIVITY RESULTS FOR VARIOUS LIG SAMPLES

Samples	Power (W)	Speed (m/min)	Conductivity (S/m)
1	1.35	0.45	250.64
2	1.5	0.54	276.70
3	1.65	0.63	293.08
4	1.8	0.72	319.95
5	1.95	0.82	367.78

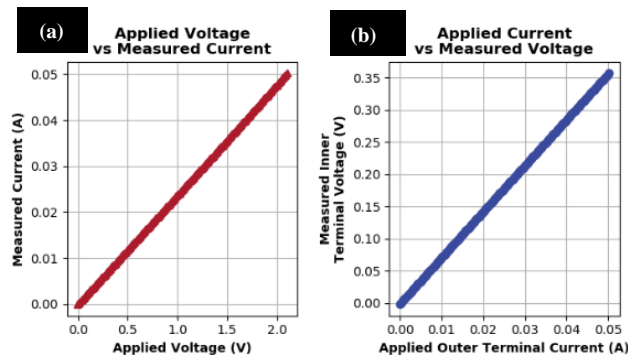


Fig 5. Measured Current vs voltage for the LIG samples

### V. Results and discussion

#### A. Capacitive Touchpad

By using AutoCAD Fusion 360, a touchpad was designed, as shown in Fig 6. The designed file was then induced with LIG on the polyimide sheet using the CO<sub>2</sub> laser machine to obtain the conductive traces. The values of the capacitance and resistance have been measured using an LCR meter. The observed values for capacitance was constant i.e. 1 pF. The

resistance values for five samples are as follows 138.3  $\Omega$ , 138.7  $\Omega$ , 140.2  $\Omega$ , 520 k  $\Omega$ , 490 k  $\Omega$ . The obtained LIG was then used as a capacitive sensor with mounted MPR121[31], which acted as a charge transfer sensing using single wire electrodes. On touching the electrode, both the capacitance and the charge transfer time increased and the microcontroller, in turn, received the information from the MPR 121, and the result for the capacitive touch sensor was displayed on the computer.

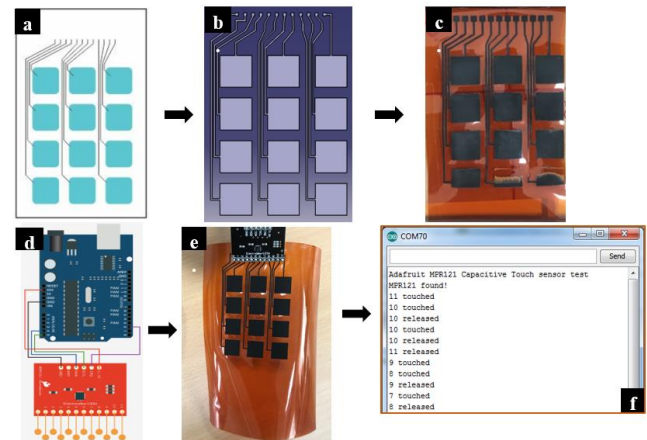


Fig 6. (a). Schematic of a touch sensor (b). CAD model of Capacitive touch sensor (c). CO<sub>2</sub> Laser Induced Graphene touch sensor on polyimide sheet (d). Schematic of Microcontroller integrated with MPR121 (e). MPR 121 mounted on LIG (f). Displaying results for Capacitive touch sensor.

#### B. Liquid-Level Sensor

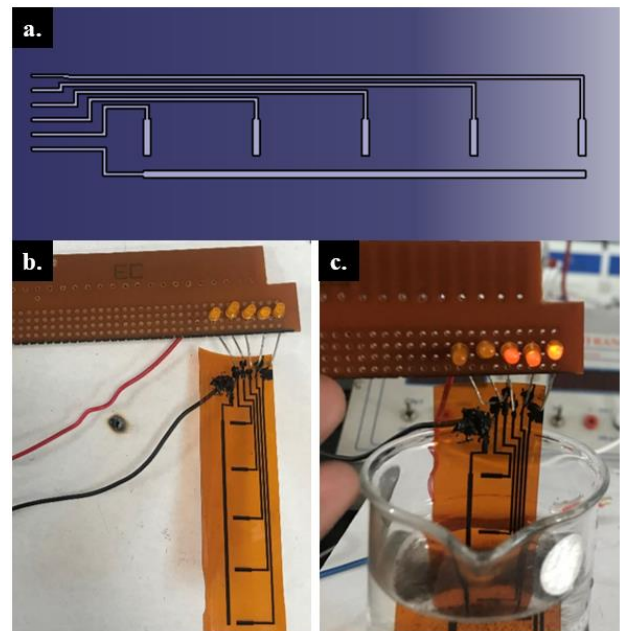


Fig 7. (a). CAD model of liquid level sensor (b). LIG arranged with LED lights on PCB (c). Testing of Liquid Level sensor with water.

A liquid level sensor has been designed in AutoCAD fusion 360, where the positive terminal/trace are in straight length, and the negative terminals/trace are joined with five intervals of a horizontal line as shown in Fig 7. Then after laser ablation on the polyimide sheet [32][33], the positive terminal and the negative terminals were arranged with five LED lights, and a

9 volts battery with 7805 regulator was incorporated to observe the function of the device.

### C. Electrochemical Detection of Hydrogen Peroxide

For analyzing the hydrogen peroxide sensing with bare LIG, as a prototype, a 3-electrode system was created with the prepared LIG as a working electrode while Ag/AgCl and platinum wire as a reference and counter electrodes, respectively. Here, a rectangular shaped pattern with dimension 50 mm x 03 mm has been fabricated. Unmodified LIG is used for electrochemical sensing of Hydrogen peroxide. Further, 500  $\mu\text{M}$  of  $\text{H}_2\text{O}_2$  was prepared in 5 mL of pH 7 phosphate buffer solution. As stated, a three-electrode system with Ag/AgCl as working, Platinum as counter is used along with LIG as working for carrying out the cyclic voltammetry experiments. The experiments were carried out at 10  $\text{mV s}^{-1}$  in a potential window of -1 to +1 V. Aparicio-Martinez et al. in 2019 reported silver modified Laser Scribed Graphene (LSG) for  $\text{H}_2\text{O}_2$  sensing using a commercial GO and a 7.9  $\mu\text{M}$  LOD was reported[34]. In the present case, GO was directly induced by laser and without any further modification, it was used for  $\text{H}_2\text{O}_2$  sensing to obtain an appreciable detection limit of 0.3  $\mu\text{M}$ . Before experiments, all the solutions were purged with high-purity nitrogen. The Cyclic Voltammetry[35] measurements were carried out in 0.2 M phosphate buffer solution (PBS, pH 7.0) at the ambient temperature in the potential window 0.0 V to -1.0 V (vs. Ag/AgCl) at a scan rate of 10  $\text{mV s}^{-1}$ . Fig 8 (a) depicts the calibration plot (b.) depicts the CV of the LIG electrode in 0.2 M PBS (pH 7.0) and with various  $\text{H}_2\text{O}_2$  concentrations (from 1  $\mu\text{M}$  to 10  $\mu\text{M}$ ).

With the successive addition of  $\text{H}_2\text{O}_2$ , the reduction current gradually increases, showing excellent electro-catalytic behavior of the fabricated LIG sensor towards hydrogen peroxide sensing. Based on the literature[36], the detection limit is theoretically calculated by using a standard formula,  $3 \times \text{Standard deviation} / \text{Slope}$ . Wherein, the standard deviation of the triplicated samples with the lowest concentration current was taken. The slope was derived from the calibration plot of the concentration effect. The detection limit of the sensor was estimated to be 0.3  $\mu\text{M}$  within a linear range from 1  $\mu\text{M}$  to 10  $\mu\text{M}$ .

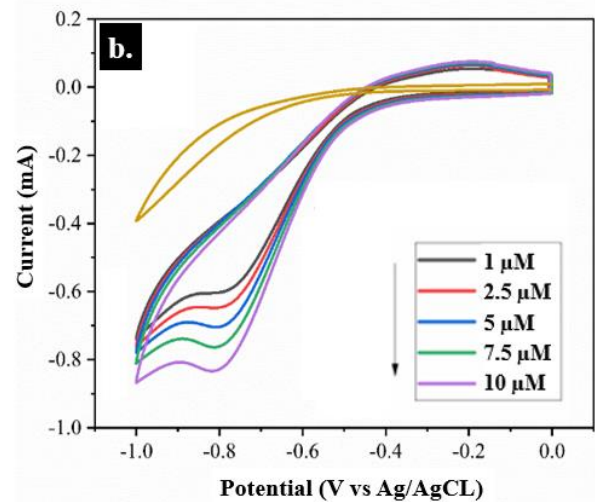
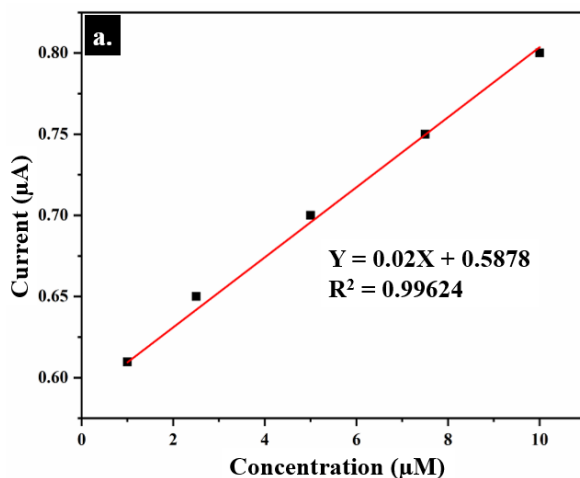


Fig 8. (a) Calibration plot of  $[\text{H}_2\text{O}_2]$   $\mu\text{M}$  vs  $\text{I}/\mu\text{A}$  (b) Cyclic Voltammetry response for different concentrations of hydrogen peroxide ( $\text{H}_2\text{O}_2$ ).

## VI. Conclusion

Herein, a single-step, cost-effective approach to realize Laser-Induced Flexible Electronic (LIFE) circuits, using low power and user-friendly  $\text{CO}_2$  laser, has been presented. Based on the design, graphene oxide (GO) has been observed to be formed on polyimide by  $\text{CO}_2$  ablation. To confirm the type of carbon allotrope, various physico-chemical characterizations, such as SEM, EDX, XPS and Raman Spectra, have been carried out. The  $\text{CO}_2$  laser parameter, such as speed and power, has been varied to optimize the conductivity of LIFE circuits. After rigorous characterizations and optimizations, experiments were carried out to explore the feasibility to test various LIFE circuits for resistive, capacitive and electrochemical sensing. With such sensing applications, the LIFE circuits have been utilized as resistive touchpads, capacitive liquid-level sensor, and electrochemical  $\text{H}_2\text{O}_2$  sensor. The Capacitive sensor, integrated with a mini-microprocessor, the functioning of the device, is proven by showing the result of glowing the LED and displaying the result of the touch sensor on the computer. For electrochemical  $\text{H}_2\text{O}_2$  sensing, the device showed a good response for various concentrations and appreciable limit of detection without any further modifications, i.e. 0.3  $\mu\text{M}$ . Overall, the LIFE devices have a strong potential to be harnessed for diverse sensing applications.

## VII. ACKNOWLEDGMENT

The authors also acknowledge Central Analytical Laboratory of BITS –Pilani Hyderabad Campus for the characterizations. The work was supported by the project (ISRO/RES/3/774/18-19) funded by RESPOND programme of the Indian Space Research Organization. Khairunnisa Amreen acknowledges DST-SERB NPDF Scheme (PDF/2018/003658) for the financial assistance.

## VIII. References

- [1] G. A. T. Sevilla *et al.*, "Decal Electronics: Printable Packaged with 3D Printing High-Performance Flexible CMOS Electronic Systems," *Adv. Mater. Technol.*, vol. 2, no. 1, 2017, doi:



- 10.1002/admt.201600175.
- [2] G. O'Grady *et al.*, "A comparison of gold versus silver electrode contacts for high-resolution gastric electrical mapping using flexible printed circuit board arrays," *Physiol. Meas.*, vol. 32, no. 3, 2011, doi: 10.1088/0967-3334/32/3/N02.
- [3] A. Petropoulos, D. N. Pagonis, and G. Kaltsas, "Flexible PCB-MEMS flow sensor," in *Procedia Engineering*, 2012, vol. 47, pp. 236–239, doi: 10.1016/j.proeng.2012.09.127.
- [4] L. Zhou, A. Wang, S. C. Wu, J. Sun, S. Park, and T. N. Jackson, "All-organic active matrix flexible display," *Appl. Phys. Lett.*, vol. 88, no. 8, pp. 2004–2007, 2006, doi: 10.1063/1.2178213.
- [5] S. Takamatsu, T. Imai, T. Yamashita, T. Kobayashi, K. Miyake, and T. Itoh, "Flexible fabric keyboard with conductive polymer-coated fibers," in *Proceedings of IEEE Sensors*, 2011, pp. 659–662, doi: 10.1109/ICSENS.2011.6127391.
- [6] Y. Cui, "Electronic Materials, Devices, and Signals in Electrochemical Sensors," *IEEE Trans. Electron Devices*, vol. 64, no. 6, pp. 2467–2477, 2017, doi: 10.1109/TED.2017.2691045.
- [7] W. Dong, X. Cheng, T. Xiong, and X. Wang, "Stretchable bio-potential electrode with self-similar serpentine structure for continuous, long-term, stable ECG recordings," *Biomed. Microdevices*, vol. 21, no. 1, 2019, doi: 10.1007/s10544-018-0353-x.
- [8] Y. A. Huang *et al.*, "Hyper-stretchable self-powered sensors based on electrohydrodynamically printed, self-similar piezoelectric nano/microfibers," *Nano Energy*, vol. 40, pp. 432–439, 2017, doi: 10.1016/j.nanoen.2017.07.048.
- [9] J. Dungan, J. Mathews, M. Levin, and V. Koomson, "Microfluidic platform to study intercellular connectivity through on-chip electrical impedance measurement," in *Midwest Symposium on Circuits and Systems*, 2017, vol. 2017-Augus, pp. 56–59, doi: 10.1109/MWSCAS.2017.8052859.
- [10] Y. Simeonov *et al.*, "3D range-modulator for scanned particle therapy: Development, Monte Carlo simulations and experimental evaluation," *Phys. Med. Biol.*, vol. 62, no. 17, pp. 7075–7096, 2017, doi: 10.1088/1361-6560/aa81f4.
- [11] A. Kaidarova, M. Marengo, G. Marinaro, N. Galdi, C. M. Duarte, and J. Kosel, "Flexible and Biofouling Independent Salinity Sensor," *Adv. Mater. Interfaces*, vol. 5, no. 23, pp. 1–6, 2018, doi: 10.1002/admi.201801110.
- [12] J. Phiri, L. S. Johansson, P. Gane, and T. Maloney, "A comparative study of mechanical, thermal and electrical properties of graphene-, graphene oxide- and reduced graphene oxide-doped microfibrillated cellulose nanocomposites," *Compos. Part B Eng.*, vol. 147, no. November 2017, pp. 104–113, 2018, doi: 10.1016/j.compositesb.2018.04.018.
- [13] B. Dai *et al.*, "Rational design of a binary metal alloy for chemical vapour deposition growth of uniform single-layer graphene," *Nat. Commun.*, vol. 2, no. 1, pp. 522–526, 2011, doi: 10.1038/ncomms1539.
- [14] Y. L. Zhong, Z. Tian, G. P. Simon, and D. Li, "Scalable production of graphene via wet chemistry: Progress and challenges," *Materials Today*, vol. 18, no. 2. Elsevier Ltd., pp. 73–78, 2015, doi: 10.1016/j.mattod.2014.08.019.
- [15] X. Dong *et al.*, "One-step growth of graphene-carbon nanotube hybrid materials by chemical vapor deposition," *Carbon N. Y.*, vol. 49, no. 9, pp. 2944–2949, 2011, doi: 10.1016/j.carbon.2011.03.009.
- [16] A. Nag and S. C. Mukhopadhyay, "Fabrication and implementation of printed sensors for taste sensing applications," *Sensors Actuators, A Phys.*, vol. 269, pp. 53–61, 2018, doi: 10.1016/j.sna.2017.11.023.
- [17] R. Ye, D. K. James, and J. M. Tour, "Laser-Induced Graphene: From Discovery to Translation," *Adv. Mater.*, vol. 31, no. 1, pp. 1–15, 2019, doi: 10.1002/adma.201803621.
- [18] Y. Chyan, R. Ye, Y. Li, S. P. Singh, C. J. Armusch, and J. M. Tour, "Laser-Induced Graphene by Multiple Lasing: Toward Electronics on Cloth, Paper, and Food," *ACS Nano*, vol. 12, no. 3, pp. 2176–2183, 2018, doi: 10.1021/acs.nano.7b08539.
- [19] J. Lin *et al.*, "Laser-induced porous graphene films from commercial polymers," *Nat. Commun.*, vol. 5, pp. 1–8, 2014, doi: 10.1038/ncomms6714.
- [20] D. A. Sokolov, K. R. Shepperd, and T. M. Orlando, "Formation of graphene features from direct laser-induced reduction of graphite oxide," *J. Phys. Chem. Lett.*, vol. 1, no. 18, pp. 2633–2636, 2010, doi: 10.1021/jz100790y.
- [21] M. R. Bobinger *et al.*, "Flexible and robust laser-induced graphene heaters photothermally scribed on bare polyimide substrates," *Carbon N. Y.*, vol. 144, pp. 116–126, 2019, doi: 10.1016/j.carbon.2018.12.010.
- [22] T. Han *et al.*, "Multifunctional flexible sensor based on laser-induced graphene," *Sensors (Switzerland)*, vol. 19, no. 16, pp. 13–22, 2019, doi: 10.3390/s19163477.
- [23] Y. Chen *et al.*, "UV Laser-Induced Polyimide-to-Graphene Conversion: Modeling, Fabrication, and Application," *Small Methods*, vol. 1900208, p. 1900208, 2019, doi: 10.1002/smt.201900208.
- [24] R. Ye, D. K. James, and J. M. Tour, "Laser-Induced Graphene," *Acc. Chem. Res.*, vol. 51, no. 7, pp. 1609–1620, 2018, doi: 10.1021/acs.accounts.8b00084.
- [25] F. Wang *et al.*, "Laser-induced graphene: preparation, functionalization and applications," *Mater. Technol.*, vol. 33, no. 5, pp. 340–356, 2018, doi: 10.1080/10667857.2018.1447265.
- [26] L. X. Duy, Z. Peng, Y. Li, J. Zhang, Y. Ji, and J. M. Tour, "Laser-induced graphene fibers," *Carbon N. Y.*, vol. 126, pp. 472–479, 2018, doi: 10.1016/j.carbon.2017.10.036.
- [27] Z. Peng *et al.*, "Flexible Boron-Doped Laser-Induced Graphene Microsupercapacitors," *ACS Nano*, vol. 9, no. 6, pp. 5868–5875, 2015, doi: 10.1021/acs.nano.5b00436.
- [28] F. T. Johra, J. W. Lee, and W. G. Jung, "Facile and safe graphene preparation on solution based platform," *J. Ind. Eng. Chem.*, vol. 20, no. 5, pp. 2883–2887, 2014, doi: 10.1016/j.jiec.2013.11.022.
- [29] F. J. Romero *et al.*, "In-depth study of laser diode ablation of Kapton polyimide for flexible conductive substrates," *Nanomaterials*, vol. 8, no. 7, pp. 1–11, 2018, doi: 10.3390/nano8070517.
- [30] A. Samouco, A. C. Marques, A. Pimentel, R. Martins, and E. Fortunato, "Laser-induced electrodes towards low-cost flexible UV ZnO sensors," *Flex. Print. Electron.*, vol. 3, no. 4, pp. 0–21, 2018, doi: 10.1088/2058-8585/aaed77.
- [31] V. Savage, X. Zhang, and B. Hartmann, "Midas: Fabricating custom capacitive touch sensors to prototype interactive objects," *UIST'12 - Proc. 25th Annu. ACM Symp. User Interface Softw. Technol.*, pp. 579–587, 2012.
- [32] Y. Kawahara, S. Hodges, N. W. Gong, S. Olberding, and J. Steimle, "Building functional prototypes using conductive inkjet printing," *IEEE Pervasive Comput.*, vol. 13, no. 3, pp. 30–38, 2014, doi: 10.1109/MPRV.2014.41.
- [33] L. Ning *et al.*, "A highly sensitive nonenzymatic H<sub>2</sub>O<sub>2</sub> sensor based on platinum, ZnFe<sub>2</sub>O<sub>4</sub> functionalized reduced graphene oxide," *J. Alloys Compd.*, vol. 738, pp. 317–322, 2018, doi: 10.1016/j.jallcom.2017.12.161.
- [34] E. Aparicio-Martínez, A. Ibarra, I. A. Estrada-Moreno, V. Osuna, and R. B. Dominguez, "Flexible electrochemical sensor based on laser scribed Graphene/Ag nanoparticles for non-enzymatic hydrogen peroxide detection," *Sensors Actuators, B Chem.*, vol. 301, no. May, p. 127101, 2019, doi: 10.1016/j.snb.2019.127101.
- [35] P. Rewatkar and S. Goel, "Next-Generation 3D Printed Microfluidic Membraneless Enzymatic Biofuel Cell: Cost-Effective and Rapid Approach," *IEEE Trans. Electron Devices*, vol. 66, no. 8, pp. 3628–3635, 2019, doi: 10.1109/TED.2019.2922424.
- [36] K. S. Shalini Devi and A. Senthil Kumar, "A blood-serum sulfide selective electrochemical sensor based on a 9,10-phenanthrenequinone-tethered graphene oxide modified electrode," *Analyst*, vol. 143, no. 13, pp. 3114–3123, 2018, doi: 10.1039/c8an00756j.
- [37] Houk Jang Yong Ju Park Xiang Chen Tanmoy Das Min-Seok Kim Jong-Hyun Ahn, "Graphene-Based Flexible and Stretchable Electronics. Adv. Mater., 28: 4184-4202. doi:10.1002/adma.201504245," *Advanced Materials*, vol. 28, pp. 4184–4202, 2016, doi: 10.1002/adma.201504245.



**Avinash Kothuru** received the B.Tech. degree in Mechanical Engineering in 2014 and the M.Tech. degree in Design for Manufacturing (DFM) from Osmania University, Hyderabad, India. During his M.tech., he worked on Design and Finite Element Analysis of BioMedical Scaffold for hard tissue and prototype

manufacturing using SLS Additive Manufacturing Technology. He Joined the Electrical and electronics Engineering Department, BITS-Pilani, Hyderabad Campus, Hyderabad, India in 2018 as a PhD candidate under the supervision of Dr. Sanket Goel, in developing Next Generation Circuit boards using Additive Manufacturing Technology with integrated Electronics and Microfluidics.



**Hanumanth Rao C.** received the M.Sc. degree in chemistry from Bangalore University, Bengaluru, India, in 1988, and the M.S. (Eng.) degree in materials science from the Indian Institute of Science, Bengaluru, in 2000.

He joined the Indian Space Research Organisation Satellite Centre, Bengaluru, in 1988, where he is currently a Manager of the High Density Interconnect (HDI) Facility. His current research interests include introduction of new technology in the field of electronic packaging miniaturization and realization of HDI and high layer count PCBs for space applications



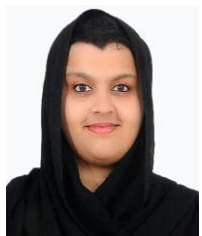
**Puneeth S. B.** received the B.E. degree in electronics and communication and the M.Tech. degree in digital electronics from Visvesvaraya Technological University, Belgaum, India, in 2013 and 2015, respectively, with a focus on low area field-programmable gate array implementation of decryption unit for AES using Vedic Math. He is currently

pursuing the Ph.D. degree with the Electrical and Electronics Engineering Department, Birla Institute of Technology and Science, Hyderabad, India, under the supervision of Dr. S. Goel, where he is developing the electro-microfluidic viscometer for various applications. He holds an Indian patent.



**Mary Salve** received the B.Tech. degree in Electronics and Telecommunication in 2016 and the M.Tech. degree in VLSI Design in 2018 from RTM University, Nagpur, India. During his M.Tech. She worked on developing PDMS based microfluidic devices for adulteration detection and cancer diagnostics. She

joined the Electrical and Electronics Engineering Department, BITS-Pilani, Hyderabad Campus, Hyderabad, India in 2018 as a PhD candidate under the supervision of Dr Prasant Pattnaik and Dr. Sanket Goel, in development of Automated IoT based Microfluidic Electrochemilumines (ECL) Biosensing platform for various biomarker detection.



**Dr. Khairunnisa Amreen** is currently working as National Post Doctorate (NPDF) for DST- SERB. She has graduated B.Sc. in three majors (Chemistry, Biotechnology and Microbiology) from Osmania University-Hyderabad (2008-2011). Post which she completed her Masters in M.Sc.

Analytical Chemistry from Vellore Institute of Technology-Vellore, Tamil Nadu, India (2011-2013). Following which she continued her Ph. D. from Vellore Institute of Technology-Vellore, Tamil Nadu, India working there as a teaching cum research associate (TRA) and CSIR-SRF in the area of Electro-analytical techniques (2013-2019) under the guidance of Dr. A. Senthil Kumar, Senior professor, VIT-Vellore. The dissertation of my research work is entitled as design and development of whole blood and heme based biosensors for electroanalytical applications. During her Ph.D. tenure she published 9 international/national research articles and filed one Indian patent for the blood based biosensor developed. Presently she is working as NPDF-DST SERB under the supervision of Dr. Sanket Goel, Head & Associate professor, EEE, BITS-Pilani, HYD.



**Sanket Goel** received the B.Sc. (H-physics) degree from Ramjas College, Delhi University, the M.Sc. (physics) degree from IIT Delhi, and the Ph.D. (electrical engineering) degree from the University of Alberta, Canada, under the NSERC Fellowship. He headed the R&D Department and worked as an Associate

Professor with the Electronics and Instrumentation Engineering Department, University of Petroleum and Energy Studies, Dehradun, India, from 2011 to 2015. He is currently an Associate Professor and Head, Electrical and Electronics Engineering Department, BITS-Pilani, Hyderabad Campus, Hyderabad, India. He has >60 publications, 6 patents (1 U.S. and 5 Indian) to his credits, delivered >50 invited talks, and guided 6 Ph.D. and 10 master's students. His current research interests are microfluidics and nanotechnology, materials and devices for energy (both conventional and renewable), and biomedical applications. He has won several awards during the course of his career, including the Prestigious Fulbright-Nehru Fellowship (2015), the Young Scientist Award (2013), the Best Students Paper Award (2005), and the Ph.D. Thesis Award (2005). Currently, he is the Associate Editor of IEEE Sensors Journal and IEEE Access, and holds visiting appointment with UiT, The Arctic University of Norway.